DOI: 10.3901/CJME.2015.0217.019, available online at www.springerlink.com; www.cjmenet.com; www.cjme.com.cn

Hot Granules Medium Pressure Forming Process of AA7075 Conical Parts

DONG Guojiang[1], ZHAO Changcai[2, *], PENG Yaxin[2], and LI Ying[2]

1 *College of Vehicles and Energy, Yanshan University, Qinhuangdao 066004, China*
2 *Key Laboratory of Advanced Forging & Stamping Technology and Science of Ministry of Education, Yanshan University, Qinhuangdao 066004, China*

Received October 11, 2014; revised February 13, 2015; accepted February 17, 2015

Abstract: High strength aluminum alloy plate has a low elongation at room temperature, which leads to the forming of its components need a high temperature. Liquid or gas is used as the pressure-transfer medium in the existing flexible mould forming process, the heat resistance of the medium and pressurizing device makes the application of aluminum alloy plate thermoforming restricted. To solve this problem, the existing medium is replaced by the heat-resisting solid granules and the general pressure equipments are applied. Based on the pressure-transfer performance test of the solid granules medium, the feasibility that the assumption of the extended Drucker-Prager linear model can be used in the finite element analysis is proved. The constitutive equation, the yield function and the theoretical forming limit diagram(FLD) of AA7075 sheet are established. Through the finite element numerical simulation of hot granules medium pressure forming(HGMF) process, not only the influence laws of the process parameters, such as forming temperature, the blank-holder gap and the diameter of the slab, on sheet metal forming performance are discussed, but also the broken area of the forming process is analyzed and predicted, which are coincided with the technological test. The conical part whose half cone angle is 15° and relative height H/d_0 is 0.57, is formed in one process at 250℃. The HGMF process solves the problems of loading and seal in the existing flexible mould forming process and provides a novel technology for thermoforming of light alloy plate, such as magnesium alloy, aluminium alloy and titanium alloy.

Keywords: granules medium, aluminum alloy sheet, drawing, hot forming, forming limit diagram

1 Introduction

Nowadays, high strength aluminum alloy sheet has become the preferred material of key components in the manufacturing fields such as aviation and aerospace etc. However, under room temperature, aluminum alloy sheet has such a poor deformation ability that its elongation is generally less than 10%–15%[1–2], thus it can be hardly used to form parts with complex cross-sectional shape, which greatly restricts its wide applications. Therefore, to solve this problem, it is imminent to develop new principles and technologies of high-properties and precision in aluminum alloy sheet thermoforming. As an advanced flexible forming method, the soft mold forming technology on sheet metal can achieve one-time forming of parts with complex shape[3].

Currently, Thermo-hydroforming process which uses liquid as the pressure-transfer medium has developed the most rapidly in the field of aluminum alloy sheet soft mold forming. In 2004, the proposal report of the United States Wright Foundation research project funded the area of thermo-hydroforming process of light alloy as a key object of the industrialization. Supported by the U.S. Department of Energy and the National Science Foundation and led by T. ALTAN from the Ohio State University, ERC/NSM conducted a large number of in-depth researches on thermo-hydroforming process of light alloy[4–5]. ABEDRABBO, et al[6], developed a temperature-dependent anisotropic material model and performed coupled thermo mechanical finite element analysis of the forming process to investigate both forming and failure behavior at elevated temperatures. MAHABUNPHACHAI, et al[7], found that the strain rate of AA5754 sheet could affect the formability of sheet metal only at high temperature. When temperature was more than 200℃, the lower strain rate could improve the bulging height of sheet metal while the higher strain rate would reduce the formability of sheet metal. Based on BARLAT 2000-2d yield criterion and Marciniak-Kuczynski(M-K) model, POURBOGHRAT, et al[8], draw the forming limit diagram of AA5754-O sheet associated with the temperature. And through process test and numerical simulation, the drawing limit of warm stamping, hydroforming and thermo-hydroforming process on sheet metal were researched. PALUMBO, et al[9], formed AA6061 bipolar plates by the thermo-hydroforming

* Corresponding author. E-mail: zhao1964@ysu.edu.cn
Supported by National Natural Science Foundation of China(Grant Nos. 51305386, 51305385), and Hebei Provincial Natural Science Foundation of China(Grant No. E2013203093)

process, and the shape of drawing parts and the process parameters were optimized by the finite element numerical simulation. Hill48 criterion and M-K model were used to construct the theoretical FLD of 5A06 Al-Li alloy by LANG, et al[10], based on the FLD, the influence laws of some key parameters, such as forming temperature, deformation velocity, thickness normal stress and inhomogeneity factor, on formability were studied. And the cylindrical parts of 5A06 Al-Li alloy with a lager draw ratio were achieved by warm hydromechanical deep drawing at 250℃.

Warm hydroforming can not only make the production of sheet parts be simple and flexible, but also reduce mold costs greatly, especially is suitable for the manufacturing of sheet metal components which are complex-shaped, size-varied, high-quality in appearance and small batch.

In addition, the quick plastic forming(QPF) process with high strain rate, short forming cycle and low cost by overall forming of parts with complex shape, is developed from the aerospace aluminum super plastic forming(SPF) process. And the QPF process is proposed mainly for high-volume production of AA5038 automotive panel, now its related products have been adopted by General Motors of United States and Honda of Japan[11–12]. On basic research, ABU-FARHA, et al[13], studied the rapid gas pressure bulging technology of AA5038 sheet under high temperature, from which the forming limit curve was obtained. Although the formability diagrams were confined to the biaxial strain region, the elliptical die insert methodology provides formability maps under conditions where traditional mechanical stretching techniques were limited. MCNELLEY, et al[14], described the plastic deformation mechanisms that were active at QPF and SPF conditions. LIANG, et al[15], obtained the best proportion of the hot forming and the superplastic forming through simulation experiment, and formed a car's a bonnet by applying the proportion. The study result shows that, the high rate superplastic forming technology can meet the requirements for mass production. The QPR process has been gradually applied in hot forming of titanium alloy and magnesium alloy[16–17]. The QPF process can be applied in larger temperature range(Strain rate is at 10^{-2} s^{-1} level), which overcomes many defects of superplastic forming, such as the low productivity, higher SPF-grade materials costs, and has the advantages of optimizing the product performance and improving the production efficiency.

Although many significant results about thermoforming of sheet parts have been achieved, the flexible application of medium and small batch products in the fields of the aviation, aerospace, military and other fields, is limited by the complex process paths and high investment in specialized equipment. Therefore, HGMF process shows its unique advantages, such as easy to operate, simple device and low cost and so on. In this process, the liquid, gas or viscous medium existing in soft mold hot forming process is replaced by the heat-resisting granules medium which is easy to fill, seal, and build pressure[18–20]. So hot forming of light alloy sheet parts can be processed on general pressure equipments, its principle is shown in Fig. 1.

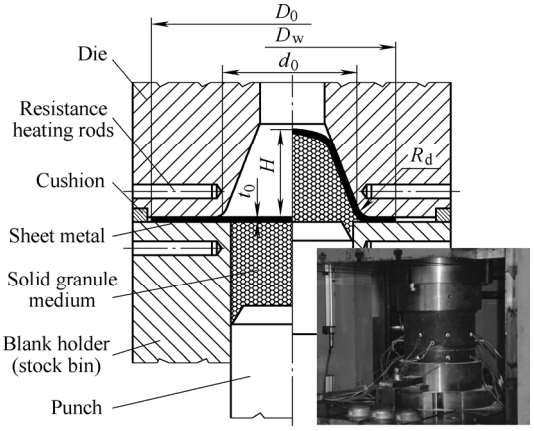

Fig. 1. Schematic diagram of HGMF on sheet metal

In order to solve the problems of liquid leakage and instability at high temperature, GRUNERAK, et al[21–22], used ceramic balls as the pressure-transfer medium to form autobody parts of high and ultra high strength steel. Also Drucker-Prager-Cap material model was used to simulate this medium. The accuracy of the numerical simulation was compared with different experiments in which the parameters were identified, and a real cup shaped part was successfully formed with granular medium. By the use of solid granule medium forming process at around 700℃, LI, et al[23], successfully formed TC1 titanium alloy spinner. The present research of the HGMF process shows that the process can adapt to a higher forming temperature by using granule medium of different materials. High pressure can be established by using general clearance seal structure. However, the HGMF process is still in the stage of basic theory research, the aluminum alloy sheet thermoforming has not been involved in the research, and arguments for the reliability of solid granules medium pressure-transfer numerical model is seldom.

Therefore, in this paper, according to property experiment of sheet material and pressure-transfer test of solid granules medium, the numerical simulation model of the HGMF process is established, the influence laws of some main process parameters on forming properties are analyzed. All above are to provide trial basis and theoretical foundation for the process.

2 Pressure-transfer Performance Test of the Solid Granules Medium

Granules medium is a discrete and frictional material[18–24], and it is different from metal, liquid and gas in constitutive relation and flow rule[25]. Based on the requirement of process, Metallic Granules(MG) or Non-metallic Granules(NMG, shown in Fig. 2) of spherical-like shape with diameters from 0.05 mm to 2 mm can be selected as the medium. As a non-cohesive material

(namely its cohesion is zero), the NMG with round and smooth appearance are selected as the pressure-transfer medium to conduct thermal deep drawing of aluminum sheet in this paper. The Rockwell hardness of this medium ranges from 48 HRC to 55 HRC. Because of the material composition, the NMG can maintain stable mechanical and chemical properties at moderate temperatures(below 400℃), which can be shown in that the NMG can keep a certain hardness and has no adhesion under high pressure.

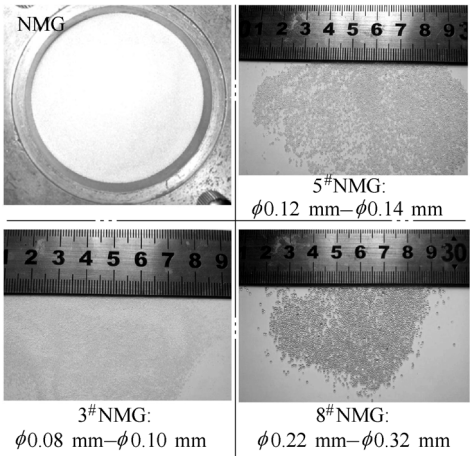

Fig. 2.　Photos of NMG

Based on the theory of granular media mechanics and rock-soil mechanics, through the uniaxial compression and shear strength tests on granular medium, the research group gained the extended Drucker-Prager linear model parameters of NMG(shown in Table 1) and the outside sliding friction coefficient f_w related to the positive pressure σ of NMG(shown in Table 2). In Refs. [18], [26]–[28], the numerical analysis of sheet and pipe forming are conducted by using the above model parameters. The result is consistent with the result of process test.

Table 1.　Extended Drucker-Prager linear model parameters of NMG

NMG No.	3#	5#	8#
Angle of friction β/(°)	26.8	31.4	33.8
Flow pressure ratio K	0.86	0.83	0.82
Dilatancy angle ψ/(°)	13.4	15.7	16.9
Drucker-prager hardening /MPa	p=926.86ε_v	p=770.44ε_v	p=465.62ε_v

Where ε_v is the volume strain, p is the average principal pressure.

Table 2.　Sliding friction coefficient of NMG

NMG No.	Fitting equation	
	0<σ<75 MPa	75 MPa≤σ<140 MPa
3#	f_w=0.047$\sigma^{0.43}$, R^2=0.996	f_w=0.30
5#	f_w=0.038$\sigma^{0.47}$, R^2=0.993	f_w=0.28
8#	f_w=0.037$\sigma^{0.44}$, R^2=0.984	f_w=0.24

2.1　Pressure-transfer test of NMG

In the test equipment, along the z-axis 12 sensors on different height positions in the sidewall of stock bin were designed for measuring the radial pressure p_r, along the r-axis another 12 sensors on different radial positions in the bottom of stock bin were designed for measuring the axial pressure p_z. During the test, the stock bin was filled with a certain volume of NMG, the load p was pressured to punch, and the signal of pressure and displacement were synchronously collected.

By filling the same volume of 5#NMG medium(the initial filling height z=245 mm) and loading different load p, the distribution curves of radial pressure p_r along the z-axis were gained, as shown in Fig. 3, the radial pressure presents an uneven distribution that it gradually decreases with the increase of the distance from the punch along the z-axis(as shown in Fig. 4). And the changing laws of the curves are very similar under the condition of different pressures. The curves of radial pressure can be accurately fitted by quadratic equation.

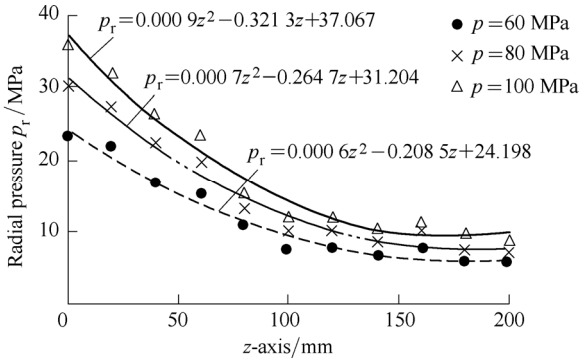

Fig. 3.　Radial pressure curve of 5#NMG

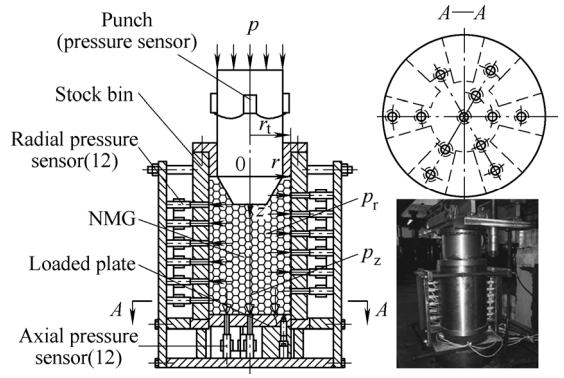

Fig. 4.　Principium of solid granules media pressure test

In order to make the test conclusions more general, the radial pressure and the z-axis coordinates can be respectively transformed as follows:

$$\alpha = p_r/p, \quad \beta = z/r_t, \tag{1}$$

where r_t is the diameter of stock bin.

As shown in Fig. 5, the corresponding data points on the α-β curves of 5#NMG at different pressures are basically coincident, which reflects the general rule of the radial pressure distribution on 5#NMG along the z-axis.

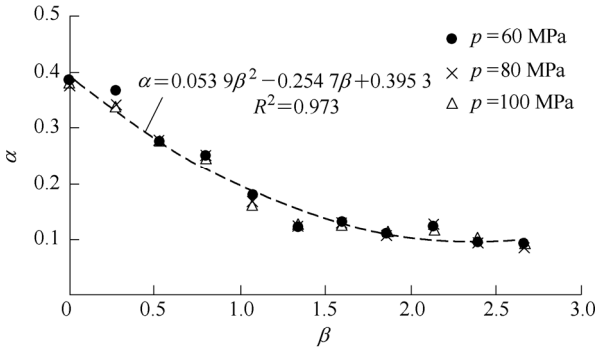

Fig. 5. α-β curve of 5#NMG

Meanwhile, the curves of the axial pressure p_z along the r-axis could be obtained under different pressures, as can be shown in Fig. 6(a), the axial pressure on the bottom of the stock bin gradually decreases from the center to the edge. The changing laws of the curves are very similar under different pressures and the bottom pressure equally increases with the increase of the punch pressure. The distribution curves of axial pressure at different initial filling height z_0 and the same pressure conditions were gained, as shown in Fig. 6(b), with the decrease of the filling height, the axial pressure on the bottom of stock bin increases and its unevenness is more significant. That is to say, the pressure loss reduces.

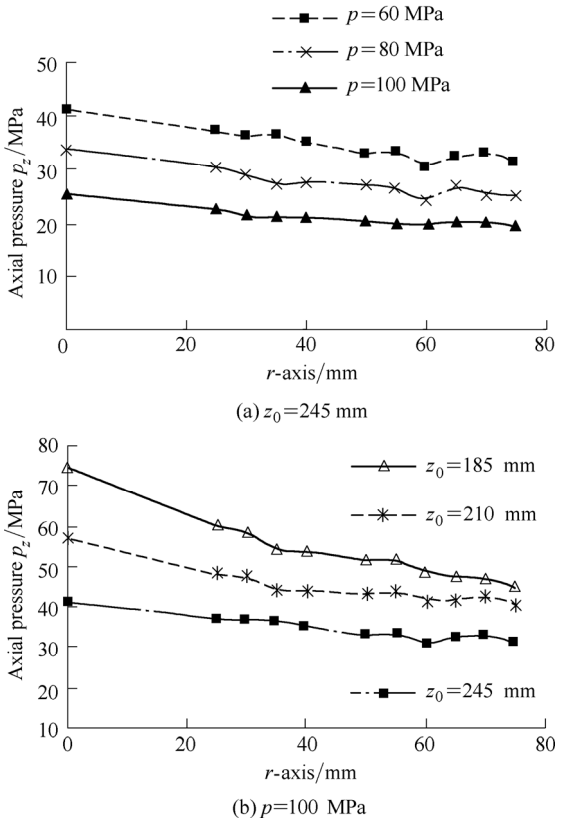

Fig. 6. Axial pressure curve of 5#NMG

The axial pressure and the z-axis coordinates can be respectively transformed as follows:

$$\chi = p_z/p, \quad \gamma = r/r_t, \tag{2}$$

The χ-γ data points of 5#NMG, which are obtained by the above transformation(shown in Fig. 7), show that the corresponding data points under the same filled height and different loading conditions almost coincide, and it can be precisely fitted by quadratic function.

$$\chi = (-0.002\,7z + 0.771\,9)\gamma^2 + (0.005\,9z - 1.651\,9)\gamma - 0.005\,5z + 1.756\,. \tag{3}$$

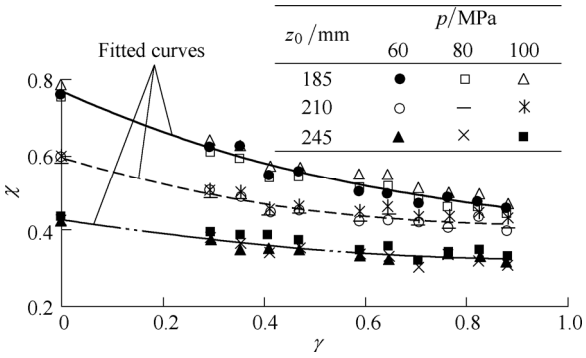

Fig. 7. χ-γ curve of 5#NMG

2.2 Numerical analysis of pressure-transfer properties on NMG

The Drucker-Prager linear model offered by the commercial finite element software ABAQUS can reflect that the compressive hardening of granular medium, the yield strength is associated with confining pressure level and the compressive yield strength is much greater than the tensile yield strength. The model can also be applied to simulate the discrete material which has the effect of internal friction in simple load condition. Based on the test data of the NMG material properties(shown in Table 1 and Table 2) and the extended Drucker-Prager linear model, the material model of NMG granular medium is established. According to the actual parameters which are obtained by pressure-transfer test, the axisymmetric numerical model is established. Taking the 5#NMG for example, by setting the initial filling height z_0=245 mm and respectively loading different pressures to the punch, the radial stress nephogram was gained, as shown in Fig. 8. The radial pressure in the wall of numerical simulation model was collected to compare with the test data, as shown in Fig. 9.

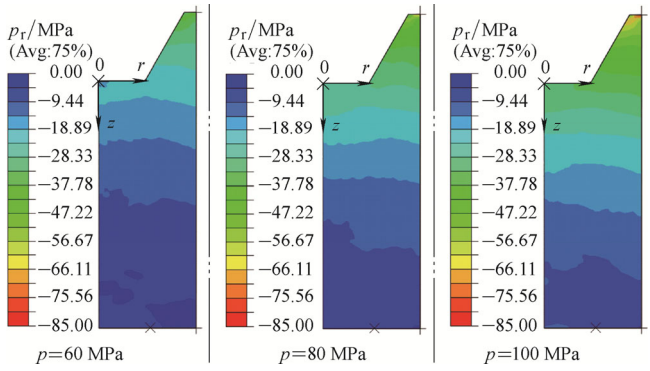

Fig. 8. Radial pressure cloud of 5#NMG

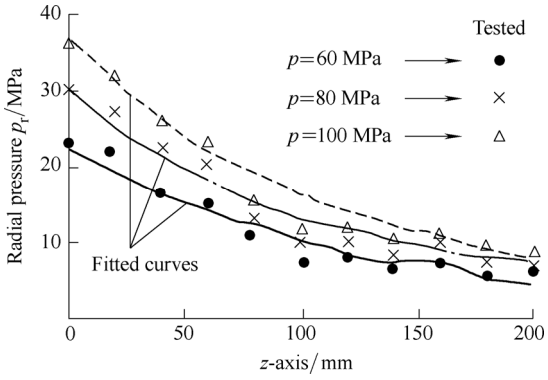

Fig. 9.　Comparison picture between simulation radial pressure curves and test radial pressure curve of 5#NMG

With the increase of the distance from the punch along the z-axis, the simulation radial pressure gradually decreases, and its decreasing amplitude increases with the increase of punch pressure. The changing laws of the radial pressure curves which gain by simulation and test are similar, as well as the decreasing amplitudes. Similarly, the axial pressure nephogram of 5#NMG is gained from the numerical simulation, as shown in Fig. 10, the internal pressure of NMG gradually decreases from the punch to the bottom and away from the central axis. With the increase of punch pressure, the decreasing amplitude of the internal pressure in NMG increases, and the volume of NMG have a certain degree of compression. The comparison result of simulation and actual measurement(as shown in Fig. 11) shows that the simulation curve is more placid than the test one, the axial pressure on the center of bottom is lower than the test value, though the difference value is slightly larger than 10%, the value are generally similar.

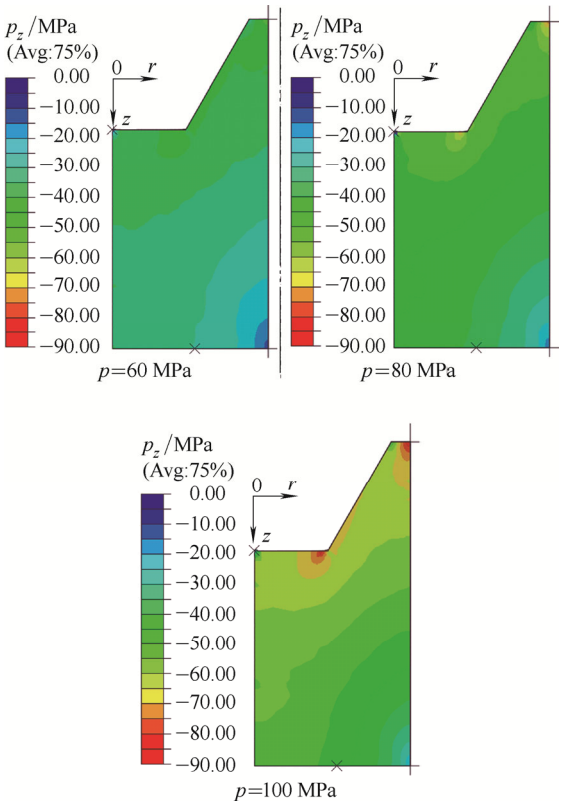

Fig. 10.　Axial pressure cloud of 5#NMG

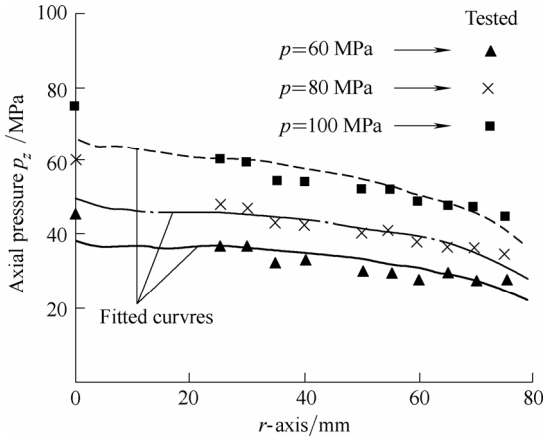

Fig. 11.　Comparison picture between simulation axial pressure curves and test radial pressure curve of 5#NMG

In conclusion, under the assumption of extended Drucker-Prager linear model, the pressure-transfer law of NMG, which mainly is based on the compressive stress, can be accurately reflected.

3　Experimental Research on AA7075 Sheet Material Properties

The ultra high strength aluminum alloy cold-rolled sheet AA7075, whose specification is 1.0 mm×1200 mm×2000 mm, is selected as the experimental material. The thermal unidirectional tensile test equipment is electronic universal testing machine-InspektTable100, and the methods of overall convective heat in closed heating furnaces and thermocouple direct contact measure are used. The highest temperature can reach 400℃, and the interior temperature error is ±1℃–5℃. The samples are produced by ultra high pressure water cutting, and its size deviation is not greater than 0.02 mm. The true stress-strain curves of AA7075 sheet under different temperatures T and strain rates were gained by testing, as shown in Fig. 12.

In the test, the AA7075 sheet shows strong temperature sensitivity, and the effect of temperature is greater than the effect of strain rate. The constitutive relation of AA7075 sheet can be accurately described by the dynamic recovery mathematical model of single increasing function. Through multiplex linear regression statistics to the test data, the constitutive equation is obtained as follows:

$$\bar{\sigma} = 791.59\bar{\varepsilon}^{0.1328}\dot{\bar{\varepsilon}}^{0.0208}\mathrm{e}^{-0.0017T}, \tag{4}$$

where $\bar{\sigma}$ is the equivalent stress; $\bar{\varepsilon}$ is the equivalent strain; $\dot{\bar{\varepsilon}}$ is the equivalent strain rate; T is the deformation temperature; K is strength coefficient; n is the strain hardening index; m is the strain rate sensitivity index; b is the temperature varying coefficient.

When the strain rate is $0.001\mathrm{s}^{-1}$ and the range temperature is 25℃–300℃, the percentage elongation at maximum force A_{gt} were all between 8.09%–12.53% (shown in Fig. 13), and before the deformation is greater

than 8%, all the samples has no necking phenomenon. Therefore, when the strain rate was 0.001s^{-1} and the engineering strain was 7%, the strain values of the samples were collected to obtain the Lankford's coefficient r, as shown in Fig. 14. The weighted average plastic strain ratio $\bar{r}$ can be accurately fitted by linear equation, the fitting equation is

$$\bar{r} = 0.0011T + 0.445\ 7. \tag{5}$$

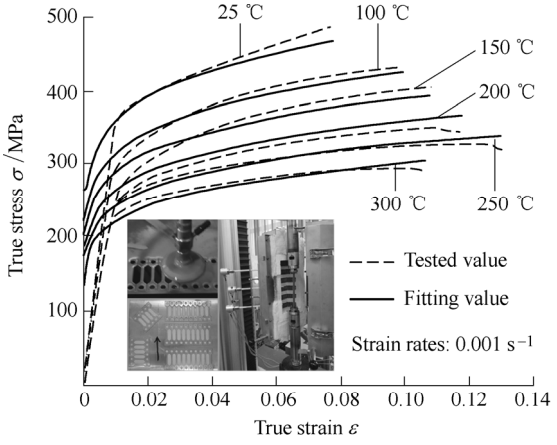

(a) Strain rate 0.001 s^{-1}

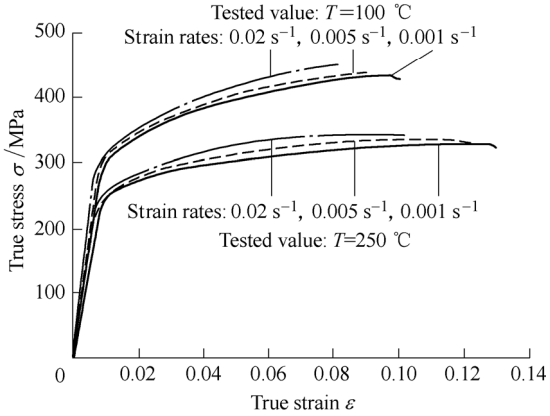

(b) T=100 ℃, T=250 ℃

Fig. 12. True stress-strain curves for AA7075 sheet

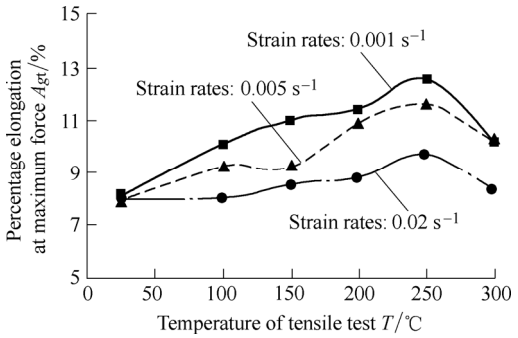

Fig. 13. Percentage elongation at maximum force curves at different temperatures and strain rates

The material properties test shows that the r-value of AA7075 sheet is larger in the moderate temperature range of 250℃–300℃, and the elongation is the largest at 250℃. It can be predicted that the best forming temperature of AA7075 sheet is around 250℃. Therefore, the forming process numerical simulation is targeting at the temperature range of 200℃–300℃.

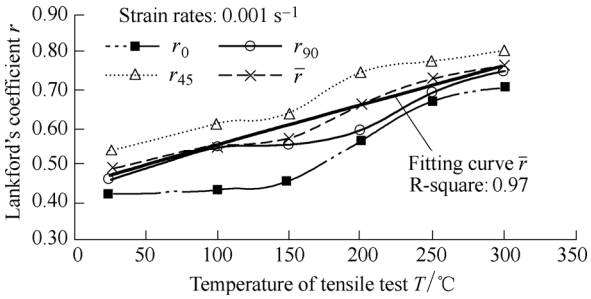

Fig. 14. Lankford's coefficient curves

Based on Hill-48 yield criterion, by using the Hill's localized necking criterion and M-K method, the theoretical forming limit diagram related to the temperature can be deduced from the constitutive equation and $\bar{r}$ -value formula which are obtained from the test, as shown in Fig. 15[29]. However, studies of many scholars show that, for the sheet material with $\bar{r}<1$, the most widely used Hill-48 yield criterion is not always suitable[30], but for the aluminum alloy sheet with $\bar{r}$ close to 1 at high temperatures, the yield characteristics can be accurately described by the Hill-48 yield criterion[29].

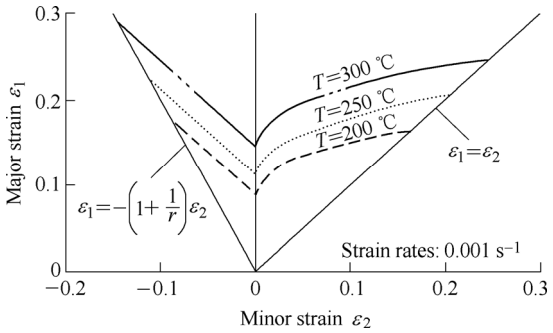

Fig. 15. Theoretical predictions of forming limit diagram

4 Numerical Simulation of HGMF Process

In this paper, taking the HGMF process forming the conical parts of AA7075 as an example, the finite element numerical simulation model is established to simulate the forming process. The sizes of target parts are shown in Fig. 16, where t_0 is the initial thickness of sheet; D_0 is the initial diameter of sheet; R_d is the entrance rounded corners of die. No dimension limits are given on forming height and bottom shape with just defining H as the free forming height. Conical parts are the typical stamping parts in deep drawing of sheet metal, and its deformation law has certain representativeness. Studies on this law can lay the foundation for searching the application of HGMF process on forming other curved surface parts.

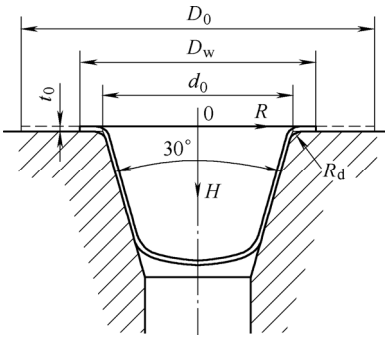

Fig. 16. Part geometry

4.1 Establishment of FEM simulation model

The simulation of HGMF, which contains a very large membrane deformation and complex frictional contact conditions, belongs to the simulation of quasi-static process. Therefore, by using the explicit nonlinear dynamic analysis method in ABAQUS/Explicit, this kind of highly nonlinear quasi-static problems can be effectively solved.

4.1.1 Axisymmetric assumption

The material properties of AA7075 sheet show that the absolute value of sheet plane directivity coefficients Δr is less than 0.17 in the temperature range of 25℃–300℃, in other words, the in-plane anisotropy is not obvious. Meanwhile, considering that the conical parts are axisymmetric rotary parts and the extended Drucker-Prager linear model using by NMG has the nature of axial symmetry, so in order to reduce the computational cost, the axisymmetric numerical model is established.

In the forming process, the model, NMG and sheet metal need to be heated to a target temperature, and the temperature needs to be maintained during loading. Therefore, ignoring the function transformation effect in the forming process, in other words, ignoring the heat exchange among model, medium and sheet metal in the numerical simulation, the forming process can be seen as isothermal deep drawing. The axisymmetric analytical rigid body model, in which the die and punch are seen as rigid bodies, is established in accordance with the actual geometry size.

4.1.2 Material model

The constitutive relation data table of AA7075 sheet can be given according to Eq. (4). Hill-48 yield criterion provided by material model library of ABAQUS and the assumptions of isotropic hardening are adopted. Sheet analysis is based on the assumptions of in-plane isotropic and normal anisotropy. The normal anisotropy parameters can be given according to Eq. (5). Based on the numerical simulation results and the theoretical forming limit diagram(shown in Fig. 15), the fracture of sheet metal in the forming process can be preliminary determined. The extended Drucker-Prager linear model is adopted as the material model of NMG, and the conditions and parameters of simulation are set according to Table 1 whose data are verified in this paper.

4.1.3 Contact conditions

Small elastic slide between the bonding contact surfaces can be allowed by penalty friction in ABAQUS, and the penalty rigidity can be automatically determined to ensure the smooth entrance from bonding state to sliding state. Thus three surface-to-surface contact pairs are separately set between mold and sheet metal, mold and medium, sheet metal and medium. The contact friction coefficient between the die and the sheet metal is set to 0.08 and those between the granule medium and the die or the sheet metal are set according to Table 2.

4.2 Simulation analysis of HGMF process

Setting the blanker holding gap(BHG) is adopted as the control method, in other words, the BHG remains unchanged in the forming process. Assuming the initial blank diameter D_0=130 mm, the initial thickness t_0=1 mm, t_G=1.15t_0, the forming temperature T=250℃, the simulation data curves under different forming stages of conical parts are obtained, as shown in Fig. 17.

The bottom free deformation region of conical parts resembles a spherical cap, and the radius of the spherical cap gradually decreases with the development of the deformation. Three feature points Z_1, Z_2 and Z_3 are selected at positions which are away from the blank center point 20 mm, 35 mm and 45 mm. By observing the movement trajectories of the feature points, we can see that point Z_1 basically moves along the vertical direction at the early and middle stages of the forming process while sharply turns to the right side at the late stage. It shows that the region from point Z_1 to the center of the bottom spherical cap sharply thins at the late stage, which can be clearly observed by Fig. 17(b). During the forming process, the bottom center of the freedom deformation region has always been the thinnest thickness point, and the thickness gradually decreases from the outer edge of the flange to the bottom center. When the forming height of the conical parts H=48 mm, the most severe thinning region is the bottom center (t=0.57 mm). According to the results of numerical simulation, the distribution curves of the major strain ε_1 and the minor strain ε_2 along the parts generatrix on the two-dimensional principal stress plane are drawn. And by inputting the theoretical forming limit curve at 250℃, the principal strain trajectories during different forming stages can be obtained, as shown in Fig. 17(c).

The change laws of those trajectories can be seen from Fig. 17(c). At the early stage of the forming process, the transition line between the free deformation region and conical surface sticking region is the closest to the fracture limit, and with the developing of the forming, the mobile trend of it toward fracture limit curve is gradually slow down. At the late stage of the forming process, the bottom free deformation region rapidly becomes another dangerous point of fracture. The principal strain trajectories of Z_1, Z_2 and Z_3 from beginning to end of the deformation are given by Fig. 17(c). When the deformation height H=40 mm, Z_2

has reached the critical region of fracture and Z_3 has been close to the fracture limit, while Z_1 is still in the safe region. Therefore it can be preliminary determined that the transition region between free deformation region and conical surface sticking region is the most dangerous region of the fracture.

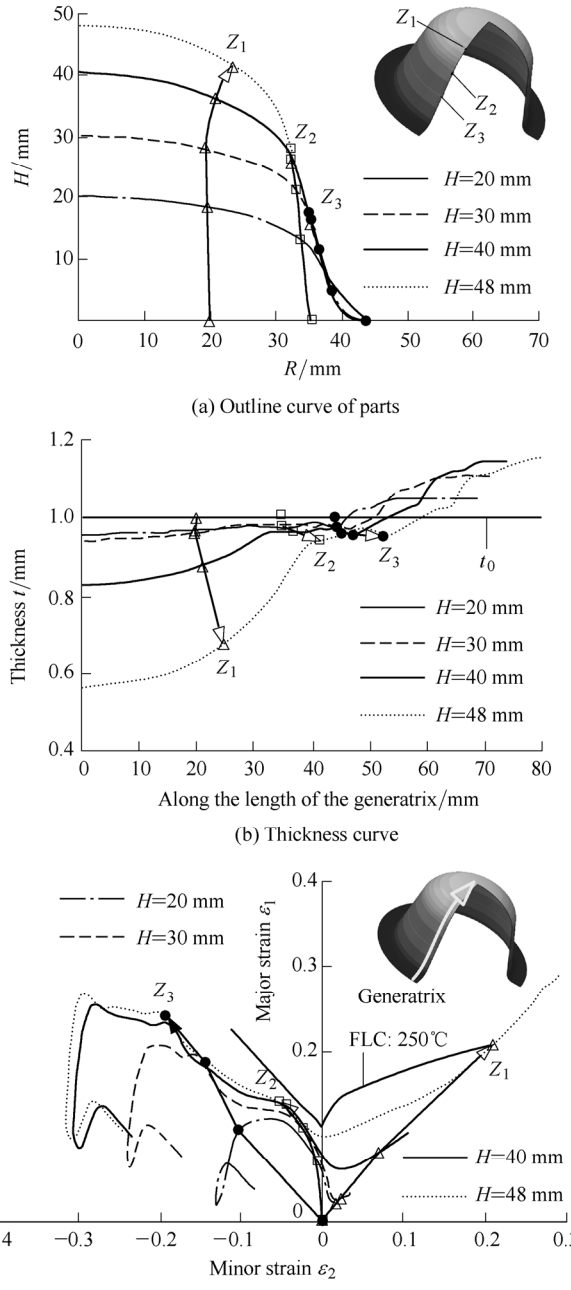

Fig. 17. Simulation data curves under different forming stages of conical parts

Case study 1: When the initial blank diameter D_0=125 mm, t_G=1.15t_0, and the deformation height H=40 mm, the principal strain trajectories at different deformation temperature are obtained, as shown in Fig. 18.

Case study 2: When the deformation temperature T=250℃, t_G=1.15 t_0, and the deformation height H=40 mm, four principal strain trajectories with the initial blank diameters are in the range of 125 mm–140 mm, are obtained, as shown in Fig. 19.

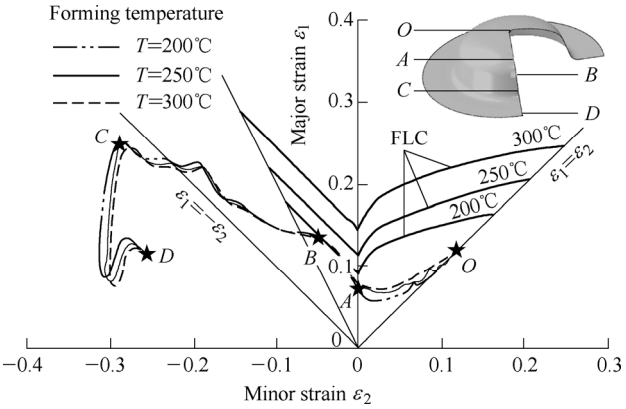

Fig. 18. Principal strain trajectories under different forming temperature (D_0=125 mm, t_G=1.15t_0)

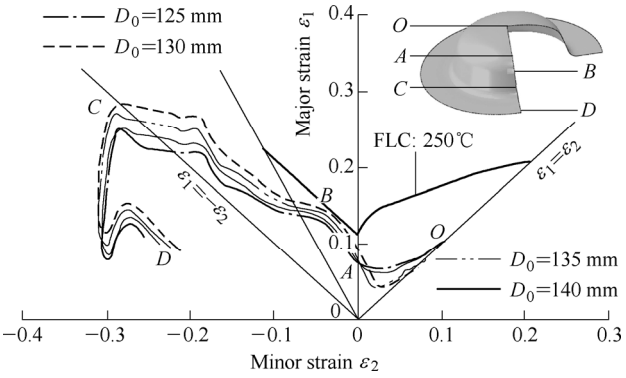

Fig. 19. Principal strain trajectories of different billet diameters (T=250℃, t_G=1.15t_0)

As shown in Fig. 18, the influence of the deformation temperature on the principal strain trajectories is not significant, especially from the plane strain state point A to the pure shear stress state point C, the principal strain trajectories basically coincide. In this range, point B which is close to unidirectional tensile state，is the closest to the dangerous point of fracture. When the deformation temperature is 200℃, this region has already exceeded the broken critical line, but for 250℃ and 300℃, the two principal strain trajectories are still in the safe region. The fracture trend of sheet metal deep drawing reduces with the rise of the deformation temperature. As shown in Fig. 19, the change of blank diameter has significant effect on the principal strain trajectories and point B is still the most dangerous point of fracture.

Case study 3: When the deformation temperature T=250℃, the initial blank diameter D_0=130 mm, the deformation height H=40 mm and the BHG are separately set with 1.10t_0, 1.15t_0 and 1.20t_0. The principal strain trajectories along the parts generatrix with different BHG are collected, as shown in Fig. 20.

The BHG has a significant effect on principal strain trajectory. If the BHG is too small, the bottom free deformation region will seriously thin with the increase of the flange resistance to deformation in the deep drawing and bulging process, and the region from point A to the

bottom center will have the risk of fracture. If the BHG is too large, point *B* in the middle section of the conic will easily become fracture danger point. It can be seen near point *B* that the principal strain trajectory with bigger BHG is closer to the fracture limit curve. The reason is that with the excessive thickening of the flange, the bending stress that makes the sheet metal flowing into the die increases, thus the deep drawing deformation resistance and the radial stress rises, as a result, point *B* flows to the fracture limit curve. Therefore, under the condition of constant BHG control, too large or too small BHG may lead fracture of the parts. Particularly, in the actual production, too large BHG can lead to the slight wrinkling of flange and further increase the frictional resistance between blank and mold, then the risk of fracture increases. Meanwhile, the surface quality of parts will be influenced by the slight wrinkle.

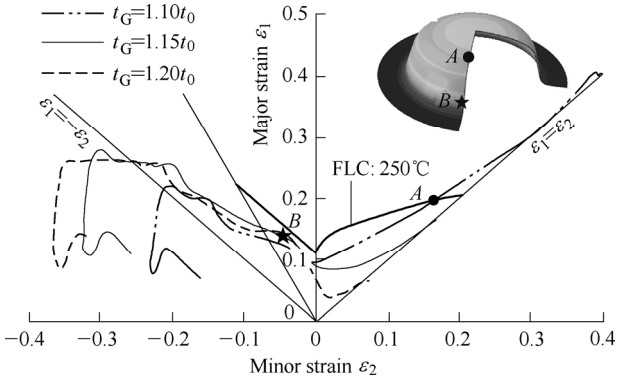

Fig. 20. Principal strain trajectories of conical part under different BHG

Based on the FEM simulation analysis of the HGMF process, the conclusion can be obtained as follow. For the AA7075 conical parts designed for this article, whose free bulging region is at the bottom, it can be preliminary determined that the blank diameter D_0 should be set in the range of 125 mm–130 mm, the temperature T should be set higher than 250℃ and the t_G=1.15t_0–1.20t_0. The conical parts with deformation height around 45 mm and thickness difference no greater than 0.33 mm can be obtained through HGMF process, and the forming force does not exceed 110 kN.

5 Research on HGMF Process Test

As shown in Fig. 1, the HGMF test mold is composed of mould base, punch, die, blank holder and blank gap adjustment device. And all die orifice diameters d_0 are 80 mm, all die orifice fillet radiuses R_d were 5 mm. Resistance heating rod is applied in temperature control system and the temperature sensors are used to achieve closed-loop controlling of heating, heat preservation and monitoring. The plate materials of AA7075 with the thickness value t_0=1.0 mm, are selected in the experiments. Ultra-high pressure water cutting technology is used to cut the plate materials into round shape blank whose size deviation is less than 0.02 mm.

In the forming process, firstly, according to process requirements, a certain volume of granular medium was filled, the blank-holder gap was set and then the mold was closed and heated. A lubricant coated plate was placed on the blank holder when the molds were open with a setting temperature, then close the molds and heat the molds to the setting temperature. After that, the punch was load by the inner slide, and at the same time, the real-time signal of pressure and displacement were collected.

Firstly, the test was to measure the impact of temperature on the forming performance of conical parts. In the experiment, the plate materials with diameters of ϕ120 mm, ϕ125 mm were selected, the t_G=1.15t_0=1.15 mm and the forming temperature was set in the range of 25℃–270℃. Under different forming temperature，the conical parts which were close to the forming limit were obtained, as shown in Fig. 21. The sheet has a poor plastic performance in the range of 25℃–230℃. The analysis of macroscopic fracture morphology shows that the positions of the fracture surfaces mainly locates in the lower parts of the die fillet entrance, and the fracture morphology of parts shows distinct brittle fracture characteristics when the temperature is below 200℃. At 200℃–230℃, the positions of the fracture surfaces mostly lie in the middle of cone wall and the transition intersecting lines between the bottom and fillet. The fracture surfaces develop along the circumferential of the parts and the fracture morphology shows ductile fracture characteristics. The fracture tendency and location coincids to the FEM simulation results, as shown in Fig. 18 and Fig. 19.

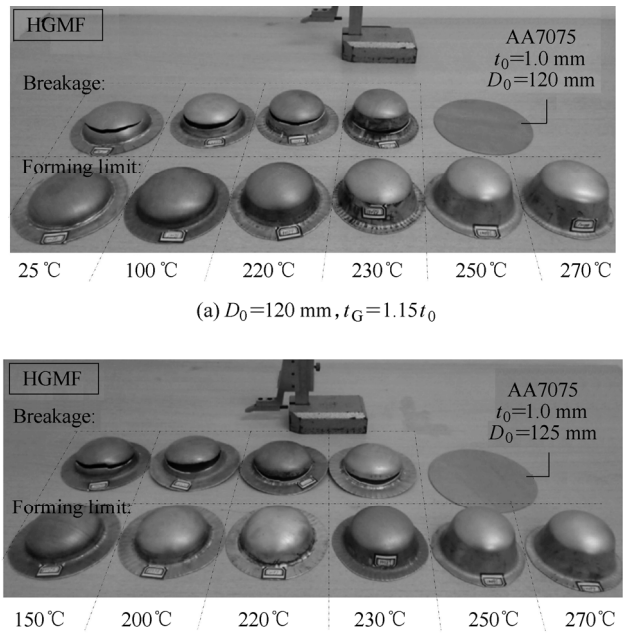

(a) D_0=120 mm, t_G=1.15t_0

(b) D_0=125 mm, t_G=1.15t_0

Fig. 21. Conical shaped pieces obtained in test under different temperature

The formability of sheet has been significantly improved and is very stable at T=250℃. The conical parts whose half

cone angle is 15° and relative height (H/d_0) is 0.57 can be formed in one time. For the parts, the surface quality of interior and exterior are good, the maximum difference of wall thickness is less than 0.4 mm, and the thinnest wall thickness is 0.72 mm which is located in bottom center of the free deformation region. The relative height of one time forming parts reaches 0.59 when the forming temperature reach 270℃, but the stability of the forming and the rate of finished products decrease, which is related to the fact that the AA7075 is a typical heat treatment material. With the forming temperature further increasing, its heat treatment state changes leading to the elongation decrease，as a result，the forming property has been influenced. The process test shows that the optimal deep drawing temperatures of AA7075 sheet are 250±20℃ when the temperature is in the range of 25℃–300℃.

Through setting the test conditions: T=250℃, D_0=125 mm, the effect of different BHG on forming performance was studied. Through repeated tests，it finds that when t_G is $1.10t_0$ or $1.20t_0$，the blank is easy to rupture during the forming process. However, the deep drawing process is stable and there is no fracture when t_G=$1.15t_0$, as shown in Fig. 22.

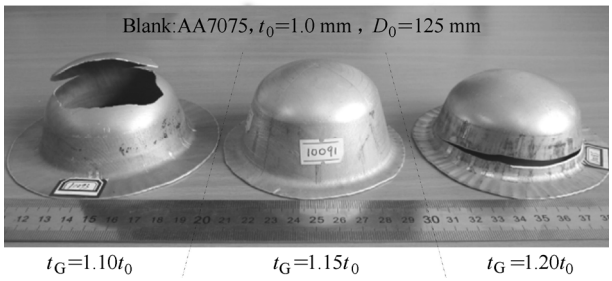

Fig. 22. Typical parts obtained in test under different BHG (T=250℃)

When t_G=$1.10t_0$, the fracture occurs at the late stage of forming, the position of the fracture surface locates at the double tensile area which belongs to the bottom of the part. Besides，the free deformation area thins seriously，the thickness of the fracture is only 0.64 mm and the outer edge diameter of the flange is 114 mm. When the blank-holder gap is too small, the deformation resistance around the flange region increases，as a result，the flange region of the sheet is difficult to satisfy the needs of deep drawing and the forming of parts more rely on the thinning of the free deformation region, therefore, serious thinning is found at the free deformation region. The drawing force continues to increase with the development of the forming. The fracture occurs when the carrying capacity of a hoop cross section at the free deformation region reaches its limit. When t_G=$1.20t_0$, the fracture occurs at the medium stage of the forming. The fracture surface locates in the middle of the conical sticking region, the thickness of the fracture is 0.84 mm and the diameter of outer flange is 106 mm. Because of the larger BHG, the sheet metal flows smoothly at the beginning of deep drawing, and the thinning of free deformation region is small. But at the middle stage of forming, the slightly wrinkling occurs at the flange region due to the overlarge BHG, and flows into the sticking area, thus the friction effect between sheet metal and the die or blank holder enhances which impedes the deformation flowing of the plate, and the forming force rapidly increases, as a result, the fracture instability occurs. At the same time, the ratio between the outer diameter of flange and the initial diameter of plate is 0.848, which is the most serious moment of the flange wrinkling in theory. The mechanics of sheet fracture instability causing by different BHG, is obtained through experiment which coincides with that in FEM simulation, as shown in Fig. 20.

In order to further verify the reliability and accuracy of the FEM simulation model on HGMF process, the typical conical parts produced by the process test were cut and measured, and then the outline curve and thickness distribution curve of the conical parts were obtained and compared with the result of numerical simulation(shown in Fig. 23). The comparison shows that the outline curve is well consistent with that obtains by FEM numerical simulation and the free deformation region at the bottom of the conical part approximates a spherical cap. The measured thickness curve is closed to the result of simulation, especially the free deformation of bottom. And the simulation result of regions from the conical surface sticking to the outer of flange is bigger than the measured value, which is no more than 8.7%.

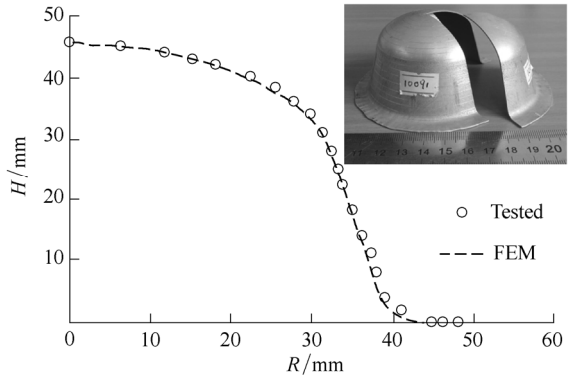

(a) Part outline

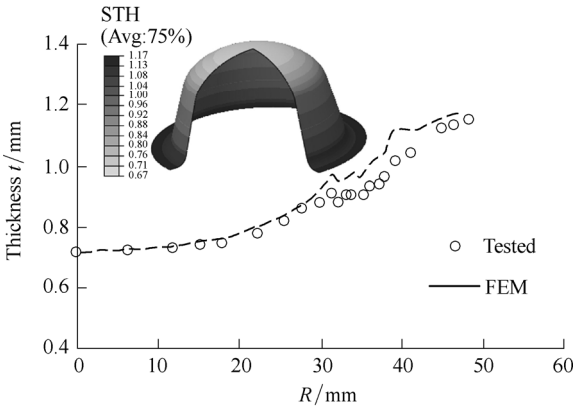

(b) Thickness distribution curve

Fig. 23. Measured values compared with simulation data of conical parts

6 Conclusions

(1) The test of solid granules medium pressure-transfer performance shows that the pressure-transfer of NMG presents a non-uniform distribution in the radial and axial, and its pressure-transfer curve can be accurately described by the quadratic equation. The extended Drucker-Prager linear model is adopted to establish the material model of NMG, by which the pressure-transfer characteristic of NMG under the condition of three-dimensional stress state can be accurately reflected.

(2) The AA7075 sheet has distinct temperature sensitivity. When the deformation temperature T=250℃ and the strain rate is 0.001s^{-1}, the elongation reaches the maximum value, namely A_{gt}=12.53%. Based on the constitutive equation obtained by test and the Hill-48 yield criterion, also with the applying of Hill's localized necking criterion and M-K method, the FLD of AA7075 sheet associated with the deformation temperature is drawn.

(3) The FEM numerical simulation model of HGMF is established, the fracture instability mechanism of AA7075 conical parts in the deformation process is analyzed, the forming parameters are optimized and the accuracy of the FEM numerical simulation forecast is proved by process test.

(4) The HGMF process test of AA7075 conical parts shows that the fracture always occurs in the lower parts of the die fillet entrance and shows significantly characteristics of brittle fracture under 200℃. In the temperature range of 200℃–230℃, the fracture always occurs in the middle of cone wall and the transition intersecting lines between the bottom and fillet，and shows significantly characteristics of ductile fracture. When the deformation temperature reaches 250℃, the deformation performance of the sheet metal can be significantly improved, and The conical parts whose half cone angle is 15° and relative height H/d_0 is 0.57, are formed in one process. At 270℃, the deformation performance begins to decline.

References

[1] JANBAKHSH M, DJAVANROODI F, RIAHI M. Utilization of bulge and uniaxial tensile tests for determination of flow pressure curves of selected anisotropic alloys[J]. *Proceedings of the Institution of Mechanical Engineers, Part L: Journal of Materials Design and Applications*, 2013, 227(1): 38–51.

[2] KUMAR M, SOTIROV N, CHIMANI C M. Investigations on warm forming of AW-7020-T6 alloy sheet[J]. *Journal of Materials Processing Technology*, 2014, 214(8): 1769–1776.

[3] YUAN S J, HE Z B, LIU G. New developments of hydroforming in china[J]. *Materials Transactions*, 2012, 53(5): 787–795.

[4] ALTAN T. Warm forming of aluminum alloys academic exercise or practical opportunity[J]. *Stamping Journal*, 2002, 14: 58–59.

[5] SHAH M, BILLUR E, SARTKULVANICH P, et al. Cold and warm hydroforming of AA754-O Sheet: FE simulations and experiments[C] //*AIP Conference Proceedings-American Institute of Physics*, Seoul, Korea, 2011, 648: 1–9.

[6] ABEDRABBO N, POURBOGHRAT F, CARSLEY J. Forming of AA5182-O and AA5754-O at elevated temperatures using coupled thermo-mechanical finite element models[J]. *International Journal of Plasticity*, 2007, 23(5): 841–875.

[7] MAHABUNPHACHAI S, KOÇ M, CARSLEY J E. Investigations on deformation behavior of AA5754 sheet alloy under warm hydroforming conditions[J]. *Journal of Manufacturing Science and Engineering*, 2011, 133: 051007–1–10.

[8] POURBOGHRAT F, VENKATESAN S, CARSLEY J E. LDR and hydroforming limit for deep drawing of AA5754 aluminum sheet[J]. *Journal of Manufacturing Processes*, 2013, 15(4): 600–615.

[9] PALUMBO G, PICCININNI A. Numerical-experimental investigations on the manufacturing of an aluminium bipolar plate for proton exchange membrane fuel cells by warm hydroforming[J]. *The International Journal of Advanced Manufacturing Technology*, 2013, 69: 731–742.

[10] LANG L H, CAI G S, LIU K N. Investigation on the effect of through thickness normal stress on forming limit at elevated temperature by using modified M-K model[J]. *International Journal of Material Forming*, 2014: 1–18.

[11] KRAJEWSKI P E, SCHROTH J G. Overview of quick plastic forming technology[J]. *Materials science forum*, 2007, 551: 3–12.

[12] SAITO K, WATANABE J, YOKOYAMA O, et al. Application technology of aluminum blow forming for automotive closure panel[C]//*Proceedings of the 6th EuroSPF Conference, Carcassonne*, France, September, 3–5, 2008: 1–7.

[13] ABU-FARHA F, HECTOR L, KRAJEWSKI P. Forming limit curves for the AA5083 alloy under quick plastic forming conditions[C]//*SAE 2011 World Congress and Exhibition*, Detroit, MI, United states, April 12, 2011: 04–08.

[14] MCNELLEY T R, OH-ISHI K, ZHILYAEV A P, et al. Characteristics of the transition from grain-boundary sliding to solute drag creep in superplastic AA5083[J]. *Metallurgical and Materials Transactions A*, 2008, 39(1): 50–64.

[15] LIANG H J, WU X W, WANG Y, et al. Research on quick superplastic forming for aluminium alloy sheet[J]. *Materials science forum*, 2013, 735: 301–306.

[16] WANG G, WANG J L, ZHANG T D, et al. Quick gas blow forming behavior of AZ31B magnesium alloy sheet[J]. *The Chinese Journal of Nonferrous Metals*, 2011, 21(9): 2023–2027. (in Chinese)

[17] SHAO Z K, HUANG Z G, JIN S Y, et al. Influence of single-direct and direct-reverse SPF on properties of TC4 alloy negative-angle parts[J]. *Journal of Aeronautical Materials*, 2013, 33(1): 1–6. (in Chinese)

[18] DONG G J, ZHAO C C, CAO M Y. Flexible-die forming process with solid granule medium on sheet metal[J]. *Transactions of Nonferrous Metals Society of China (English Edition)*, 2013, 23(9): 2666–2677.

[19] DONG G J, ZHAO C C, CAO M Y. Process of back pressure deep drawing with solid granule medium on sheet metal[J]. *Journal of Central South University*, 2014, 21(7): 2617–2626.

[20] DU B, ZHAO C C, DONG G J, et al. Study on thin-walled tube forming by solid granule medium forming[J]. *ICIC Express Letters*, 2014, 8: 2649–2654.

[21] GRÜNER M, MERKLEIN M. Consideration of elastic tool deformation in numerical simulation of hydroforming with granular material used as a medium[J]. *Key Engineering Materials*, 2011, 473: 707–714.

[22] GRÜNER M, MERKLEIN M. Numerical simulation of hydro forming at elevated temperatures with granular material used as medium compared to the real part geometry[J]. *International Journal of Material Forming*, 2010, 3(1): 279–282.

[23] LI P L, ZHANG Z, ZENG Y S. Studty on titanium alloy spinner based on solid granules medium forming[J]. *Forging & Stamping Technology*, 2012, 37(5): 60–63. (in Chinese)

[24] LADE P V, ABELEV A V. Characerization of cross-anisptropic soil deposits from isotropic compression tests[J]. *Soils and Foundations*, 2005, 45(5): 89–102.

[25] LADE P V. Failure criterion for cross-anisotropic soils[J]. *Journal of Geotechnical and Geoenvironmental Engnering, ASCE*, 2008, 134(1): 117–124.
[26] CAO M Y, ZHAO C C, DONG G J, et al. Mechanical analysis of deep drawing of cylinder based on solid granules medium forming technology[J]. *Journal of Mechanical Engineering*, 2013, 49(2): 42–48. (in Chinese)
[27] DU B, ZHAO C C, LIU Y J, et al. Research on different patterns of tube bulging process[J]. *Journal of Mechanical Engineering*, 2014, 50(16): 126–134. (in Chinese)
[28] DONG G J, ZHAO C C. Study on the forming of box-shaped parts based on solid granule medium forming[J]. *Journal of Mechanical Engineering*, 2012, 48(22): 72–79. (in Chinese)
[29] CHU X R, LEOTOING L, GUINES D, et al. Temperature and strain rate influence on AA5086 forming limit curves: experimental results and discussion on the validity of the M-K model[J]. *International Journal of Mechanical Sciences*, 2014, 78: 27–34.
[30] NAKA T, NAKAYAMA Y, UEMORI T, et al. Effects of temperature on yield locus for 5083 aluminum alloy sheet[J]. *Journal of Materials Processing Technology*, 2003, 140: 494–499.

Biographical notes

DONG Guojiang, born in 1978, is currently an associate professor at *College of Vehicles and Energy, Yanshan University, China*. He received his PhD degree from *Yanshan Universtiy, China*, in 2014. His main research direction is special forming technique of tube and panel.
Tel: +86-335-8074682; E-mail: dgj@ysu.edu.cn

ZHAO Changcai, born in 1964, is currently a professor and a PhD candidate supervisor at *Key Laboratory of Advanced Forging & Stamping Technology and Science of Ministry of Education, Yanshan University, China.* His main research direction is special forming technique of tube and panel.
E-mail: zhao1964@ysu.edu.cn

PENG Yaxin, born in 1988, is currently a master candidate at *Key Laboratory of Advanced Forging & Stamping Technology and Science of Ministry of Education, Yanshan University, China.*
E-mail: 739295573@qq.com

LI Ying, born in 1989, is currently a master candidate at *Key Laboratory of Advanced Forging & Stamping Technology and Science of Ministry of Education, Yanshan University, China.*
E-mail: 757675889@qq.com